

Fabrication and Determination of the Sun Protection Factor and Ultraviolet Protection Factor for Piscean Collagen/Bis(chalcone Derivative (B1) Composite Films with Wide-Range UV Shielding

Niveditha Nagappa Bailore, Balladka Kunhanna Sarojini,* and Kishori Ramachandra Harshitha



Cite This: *ACS Omega* 2022, 7, 27876–27885



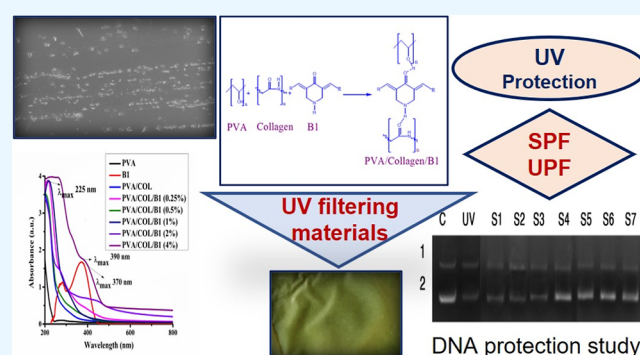
Read Online

ACCESS |

Metrics & More

Article Recommendations

ABSTRACT: The present study investigates the development of distinct UV-A and UV-B radiation filtering materials through the introduction of a heterocyclic bis(chalcone derivative [(3,5-bis{4-(methylsulfanyl)phenyl}methylidene)piperidin-4-one] (B1) into the matrix of PVA/Piscean collagen blend films (1:1) prepared through the solution casting method and characterized. The dopant concentration varied from 0.25 to 4%. The scanning electron microscopy images showed the rough surface due to the uniform dispersion of dopant B1. The addition of different concentrations of B1 altered the mechanical strength with a proportional increase in Young's modulus (146–317 MPa), tensile strength (23.3–39.21 MPa), and decrease in its elongation at break (158.8–105.2%). As the dopant B1 belongs to the bis(chalcone class of compounds which absorb in the UV–vis region (370 nm λ_{\max}) due to the α , β unsaturated keto group, it was selected for doping. Dopant concentration-dependent increase in density was observed in films (31–162 mg/cm³). The bathochromic shift in UV absorption from 370 to 390 nm for λ_{\max} as well as hyperchromism was evidenced with proportional increase in the concentration of B1, indicating its capacity to block UV rays. On determining the UV filtering ability for all the prepared films, the one with 4% dopant showed a higher sun protection factor (SPF) with a value of 27.53 and ultraviolet protection factor (UPF) with a value of 58.23. In addition, the degradation of supercoiled PBR322 DNA on UV irradiation was effectively inhibited by these films with a dopant concentration of 0.5–4.0%, which might cause less harm to the skin. The inferences of the experiments would indicate the use of these water-insoluble films as UV blocking potential materials with a merit of SPF and UPF characteristics.



1. INTRODUCTION

For many years, plastics such as polyethylene, polystyrene, polyethylene terephthalate, and polypropylene have been widely used in the packaging industry. However, the disposal of these materials after their end use requires hundreds of years to degrade in environmental conditions. Therefore, there had been an intensifying research for new materials with high performance and at an inexpensive cost that can be defined by recyclability, renewability, and biocompatibility. These polymers were starch, cellulose, chitosan, clay, pectin, collagen, gelatin and polyvinyl alcohol (PVA), eudragit, and so forth.^{1–4} The Piscean collagens were extracted from marine or freshwater fishes. They have several advantages over mammalian collagen such as easy extractability, low cost, and devoid of a religious barrier. It was reported that the Fish Collagen Peptide Market size would exceed USD 685 Million in 2020 and was estimated to register over 5.5% compound annual growth rate between 2021 and 2027.⁵ Increasing acceptance of fish collagen peptide as an animal-based ingredient in nutraceuticals and food and beverage industry is expected to propel the market growth. Of late, the

word cosmeceuticals is coined to illustrate the medicinal use of a cosmetic product. Many skin care products based on collagen blended with compounds of medicinal value are being marketed. The products which protect skin from damage due to the exposure of sun rays are listed under cosmeceuticals. The degradation of collagen leads to wrinkles that accompany aging. Continuous UV radiation from the sun reduces the production of type I collagen which is the major structural protein found in human skin, the reduction of type I collagen and it causes premature skin aging which is associated with skin carcinoma.⁶ Therefore, photoprotection is required for the skin to prevent damages. The UV filters used are divided into two classes based on the nature of working. The inorganic filters reflect light are

Received: February 7, 2022

Accepted: July 20, 2022

Published: August 4, 2022



called physical filters, whereas organic UV filters absorb light and termed as chemical filters. Usually, the physical UV filters contain metallic oxides, such as ZnO, TiO₂, and CuO which provide better protection than the chemical filters as they are insoluble in water. However, their film forming nature on the skin was not well accepted by the consumers, also making formulations was difficult as they tend to break emulsions. On the other hand, chemical UV filters usually exhibit high absorbance in the UV region due to the presence of chromophoric groups such as single or multiple aromatic rings, often in conjugation with carbon carbon double bonds and/or carbonyl moieties. After rigorous toxicological evaluations, they are put into the market. The accepted class of UV filtering materials in practice are the following: benzophenone derivatives, *p*-aminobenzoic acid and its derivatives, salicylates, cinnamates, camphor derivatives, triazine derivatives, benzotriazole derivatives, benzimidazole derivatives, and others.⁷

The blends of natural and synthetic polymer stand for an innovative class of materials with better biocompatibility and mechanical properties than those of single-component.^{8–10} The PVA is a water-soluble synthetic polymer and is biocompatible, biodegradable, non-toxic, and odorless. It also possesses high mechanical strength and chemical resistance. By blending collagen with PVA, weak properties of collagen such as poor mechanical strength and fast biodegradation rate could be overwhelmed.¹⁰ The pigment responsible for tanning of the skin is melanin, though it helps in protecting the skin from UV-induced DNA degradation, the abnormal accumulation of melanin due to higher tyrosinase activity results in uneven patches on the skin causing an aesthetic problem. Therefore, natural tyrosinase inhibitor curcumin is one of the choices as a skincare ingredient in cosmetic products. The bischalcones, synthetic curcuminoids were found to absorb UV radiations and also inhibited tyrosinase enzyme activity which equal the property of curcumin with a better solubility profile.¹¹ They exhibited promising antiviral, radioprotective, and antiangiogenic properties.^{12,13} In addition to being used in pharmaceutical industries, chalcones also find wide applications in dyes and cosmetic compositions.^{14,15} Based on the previous work from our group on bischalcone derivatives as optical materials,^{15–19} it was thought to fabricate eco-friendly films of PVA/collagen blend doped with heterocyclic chalcone [3,5-bis{[4-(methylsulfanyl)phenyl]methylidene}piperidin-4-one (**B1**)] to study the UV enduring property. Therefore, the study aimed to prepare PVA/collagen/**B1** blend films where the acid-soluble collagen (ASC) was isolated from the skin of Indian oil sardine (*Sardinella longiceps*).²⁰

2. EXPERIMENTAL SECTION

2.1. Materials. The fish Indian oil sardine was collected from a market in Mangalore. The skin portions of the fishes were removed and washed with cold distilled water and stored at –20 °C for further use. Chemicals used in the study such as acetic acid (M.W. 60.05 g/mol, 0.5 M in water), butanol (M.W. 74.12, 10% w/v in water), ethylenediaminetetraacetic acid disodium salt (M.W. 372.24, 0.5 M in water), tris (hydroxymethyl) aminomethane (M.W. 121.14, 0.05 M), and PVA of M.W. 60,000–1,25,000, Alcoholysis degree of PVA is 98–99%, 2% w/v in water, were procured from Merck, India. The bischalcone derivative [3,5-bis{[4-(methylsulfanyl)phenyl]methylidene}piperidin-4-one (**B1**)] was synthesized, purified, and characterized at Research laboratory, Industrial Chemistry, Mangalore University, Karnataka, India.¹⁵

2.2. Fabrication of the PVA/Collagen/B1** Composite Films.** The isolated ASC from the skin of Indian oil sardine (*S. longiceps*) was taken for the study using the method reported by Nagai and Suzuki (2000a) with a little modification. Amicon Ultra centrifugal filters (Millipore) 100 kDa cutoff filters were used for concentrating the proteins. The isolated collagen was characterized by scanning electron microscopy (SEM), Fourier transform infrared spectroscopy (FTIR), thermogravimetric analysis (TGA), and UV analysis. The protein patterns of the isolated collagen sample was analyzed using sodium dodecyl sulfate-polyacrylamide gel electrophoresis according to the method of Laemmli using 10% resolving gel and 6% stacking gel.²⁰ The PVA acts as a base matrix for the preparation of PVA/collagen blend films doped with different concentrations of **B1** by the solution casting method. PVA was dissolved in double distilled water and collagen solution was prepared by acetic acid (A.R. Grade). Different concentrations of **B1** (0.25, 0.5, 1, 2, and 4%) (w/v) was dissolved in dimethyl sulfoxide were added to PVA (2%)/collagen (2%) blend solution and it was stirred at 4 °C (350 rpm) for 12 h on a magnetic stirrer, further sonicated for 5 min, and it was uniformly poured onto the Petri plate as a thin film and dried at 40 °C for 24 h. The films were cooled to room temperature, slowly peeled off from the Petri plate and stored in a polyethylene bag.

2.3. Instrumental Analysis. Structural confirmation of **B1**-doped PVA/collagen-fabricated composite films was carried out using FTIR spectroscopic analysis (between 4000 and 500 cm⁻¹) by using a Shimadzu FTIR instrument (Model: IR Prestige-21, Shimadzu Corporation, Japan). The surface morphology of the films was analyzed by a field emission scanning electron micrograph (Carl Zeiss Microscopy Ltd). TGA was carried out to analyze the thermal decomposition of fabricated films by using TA instruments (Model; SDTQ600, TA Instruments, UK). The thermal scanning was carried out at a uniform scanning rate of 10 °C/min over the temperature range of 25–700 °C. Mechanical properties of the nanocomposite films were measured by using Zwick & Roell 2020 (Loadcell 100 N) testing machine with a test speed of 12.5 mm/min. The mechanical property was done in Konkan Specialty Poly products Pvt Ltd, KIADB Industrial Area, Baikampady Mangalore. The sun protection factor (SPF) and ultraviolet protection factor (UPF) was calculated based on UV absorbance and transmittance values obtained from a spectrophotometer (Spectroquantpharo 300) at the UV region (290–400 nm).

2.4. Density of the Cross-Linked Composite Film. The density of all prepared cross-linked film samples were analyzed using the liquid displacement method with ethanol as a liquid.^{21,22} At first, a known weight (*W*) of the sample (35 mg) was immersed in a graduated cylinder containing a known volume (*V*₁) of ethanol for 15 min. The volume of ethanol with the sample was measured (*V*₂). Then, the sample was removed from the cylinder, and the volume of ethanol (*V*₃) was also recorded. Volumes of each of samples were measured in triplicates. Density was calculated by the following equation

$$\text{Density} = W / (V_2 - V_3)$$

2.5. *In vitro* SPF Determination of the Fabricated Films. The SPF of the fabricated films was determined through UV absorbance value as calculated from the Mansour equation.^{23–25}

$$\text{SPF} = \text{CF} \sum_{290}^{320} \text{EE}(\lambda) \times \text{I}(\lambda) \times \text{Abs}(\lambda)$$

where CF = correction factor (10), EE = erythrogenic effect of radiation with wavelength λ , I = solar intensity spectrum, and Abs(λ) = spectrophotometric absorbance values at wavelength.

Where the prepared composite films were scanned between 290 and 320 nm by using a UV spectrophotometer and the obtained absorbance values were multiplied with the respective EE (λ) and I (λ) values (constant value as shown in Table 1).²⁶ Then, their summation was taken and multiplied with the correction factor (10).

Table 1. Values of EE (λ) x I at Different Wavelengths

Wavelength (λ nm)	Value of EE (λ) x I (λ) (normalized)
290	0.0150
295	0.0817
300	0.2874
305	0.3278
310	0.1864
315	0.0837
320	0.0180

The percentage of UV protection is equal to 100-(100/SPF).²⁷

2.6. In vitro UPF Determination of Fabricated Composite Films. The procedure used for UPF determination by the in vitro method was reported by Cunha et al., and the standard mentioned was Australia/New Zealand standard, AS/NZS 4399:1996.²⁸ The UPF is a standard used to measure the effectiveness of sun-protective fabrics. It provides both UV-A and UV-B radiation protection. An *in vitro* method of determining UPF of the fabricated films was calculated through the UV transmittance value by UV-vis spectroscopy. The transmittance data were used to calculate the UPF using the following equation.²⁹

$$\text{UPF} = \frac{\sum_{290}^{400} \text{E}(\lambda) \text{S}(\lambda) \text{d}(\lambda)}{\sum_{290}^{400} \text{E}(\lambda) \text{S}(\lambda) \text{T}(\lambda) \text{d}(\lambda)}$$

where E(λ) is the relative erythema action spectrum, S(λ) is the spectral irradiance ($\text{W m}^{-2} \text{nm}^{-1}$), T(λ) is the average spectral transmittance of fabric, d(λ) is the bandwidth, and λ is the wavelength.

The percentage blocking for UV-A (320–400 nm) was calculated by using the following equation,²⁹

$$\text{UV A blocking (\%)} = 100 - \frac{\sum_{320}^{400} \text{T}(\lambda) \text{d}(\lambda)}{\sum_{320}^{400} \text{d}(\lambda)}$$

The percentage blocking for UV-B (280–320 nm) was calculated by using the following equation

$$\text{UV B blocking (\%)} = 100 - \frac{\sum_{280}^{320} \text{T}(\lambda) \text{d}(\lambda)}{\sum_{280}^{320} \text{d}(\lambda)}$$

After the estimation of SPF and UPF, the possible use of these developed films in cosmetic as well as textile industries demanded their toxicity assay. Therefore, protection of DNA degradation by these fabricated films was undertaken.

2.7. In vitro DNA Degradation Study of the Fabricated Composite Film. In a 96-well plate, supercoiled PBR322 (4361

bp) about 200 ng was treated in Tris buffer (5 mM Tris-HCl, 50 mM NaCl, pH 7.2) to yield a total volume of 10 μL . The well containing this mixture was covered with different membrane samples and then UV irradiated at a wavelength of 365 nm for 1 h at 37 $^{\circ}\text{C}$. The reaction was quenched by the addition of 3 μL loading buffer, and then, the resulting solutions were loaded on a 1% agarose gel. Electrophoresis was carried out at 80 V for 1 h in TAE buffer (pH 8.0). The DNA bands were visualized under UV light and photographed.

3. RESULTS AND DISCUSSION

3.1. Composite PVA/Collagen/B1 Film Synthesis. The ASC blended with PVA was to increase the thermal stability and to strengthen the film upon which resulted in good quality films. The PVA contains considerable amounts of hydroxyl groups and also the hydroxyproline component of collagen act as hydrogen donors, whereas amide linkage $-\text{NH}-\text{C}=\text{O}-$ would acts as acceptors in a polymer matrix.³⁰ Upon the addition of **B1**, the stable composite films were formed. The compound **B1** is polar in nature with $-\text{C}=\text{O}-$ and $-\text{NH}-$ groups of the piperidone core. Therefore, strong interaction formed between dopant and matrix by non-covalent interaction of hydrogen bond type (Figure 1a,b). The characteristics of the developed films (Figure 2) with varying concentrations of **B1** were determined for noting the change in physicochemical properties.

3.2. Field Emission Scanning Electron Microscopy Analysis. The microscopy of surface changes in the PVA and

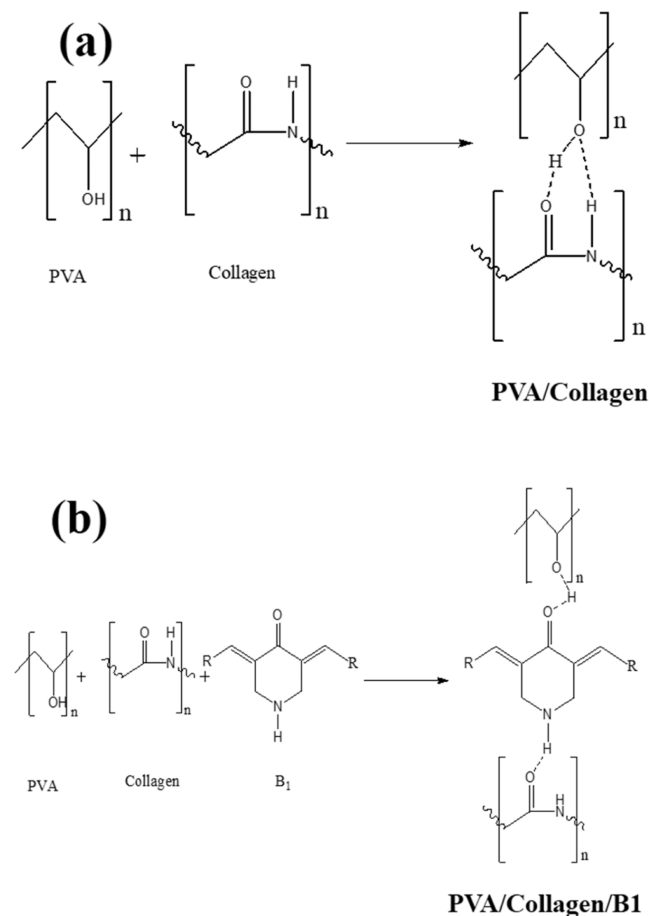


Figure 1. Plausible hydrogen bonding between (a) PVA/collagen and (b) PVA/collagen/B1.

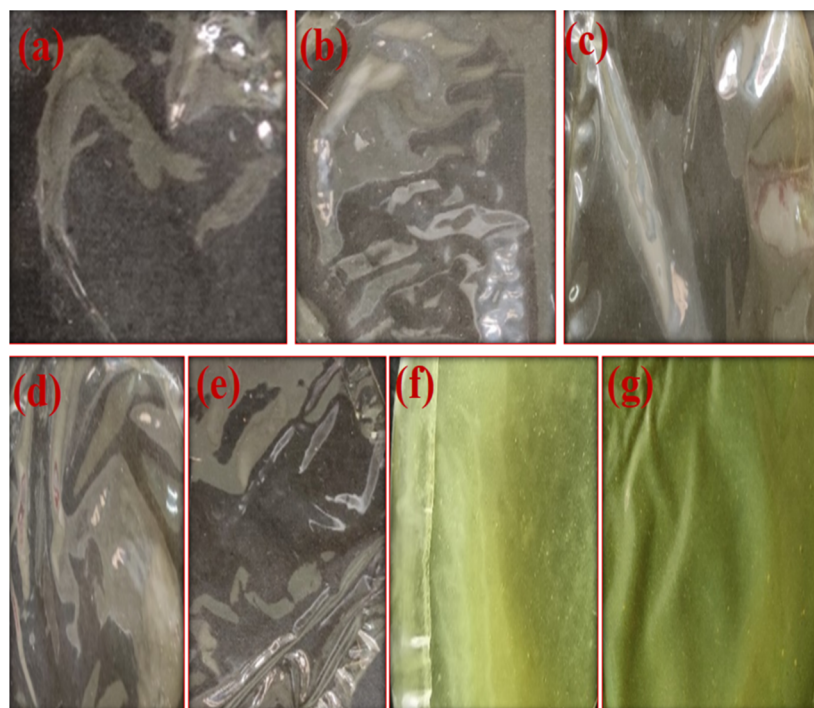


Figure 2. Different concentrations of B1-doped PVA/collagen films: (a) PVA (2%), (b) PVA (2%)/collagen (2%), (c) PVA/collagen/B1 (0.25%), (d) PVA/collagen/B1 (0.5%), (e) PVA/collagen/B1 (1%), (f) PVA/collagen/B1 (2%), and (g) PVA/collagen/B1 (4%).

PVA/collagen blend film doped with different concentrations of B1 is shown in Figure 3a–g. The pure PVA film was uniform in composition and the film looks smooth, indicating its amorphous nature. When collagen was mixed with PVA it showed a dense fibrous morphology, as shown in Figure 3a,b. The SEM analysis of different concentrations of B1-doped composite films showed that there was a gradual change in morphology as the dopant concentration increased. The dopant crystals were distributed as microcrystals in the PVA/collagen matrix. It could be observed that as the concentration of B1 ranged from 0.25 to 4%, the dopant was uniformly dispersed and embedded in the polymer matrix. It was also observed that the dopant strongly adhered to the matrix which exhibited modification in the physical and chemical characteristics of the film.

3.3. FTIR Analysis. The interaction between PVA/collagen/B1 blended films was investigated using FTIR, as shown in Figure 4a–g.

Figure 4a represents the pure PVA film with a broad –OH stretching vibrations band between 3304 and 2924 cm^{-1} which could be attributed to the –C–H stretching vibration band. The –C=O stretching vibration of the PVA backbone was observed at 1720 cm^{-1} . The –C=O carbonyl stretching vibration was observed at 1652 cm^{-1} .^{18,31,32}

Figure 4b represents the PVA/collagen blend film indicated the formation of hydrogen bonding between PVA and collagen. The broad bands at 3280 cm^{-1} (Amide A, the stretching of –N–H and –O–H) confirmed the presence of collagen in the PVA matrix, where –N–H stretching vibration of the amide A band and also due to the hydroxyl group (–O–H) of the PVA matrix which indicated the presence of a hydrogen bond between the PVA and collagen. The band at 2922 cm^{-1} which could be attributed to the –C–H stretching vibration. The band at 1646 cm^{-1} was related to the –C=O stretching (Amide I), the absorption band appeared at 1550 cm^{-1} (Amide II) might be

due to the bending vibration of the –N–H group coupled with the –C–N stretch. The absorption band appeared at 1323 cm^{-1} might be due to –CH₂ wag of proline and glycine. The PVA/collagen blend gave a strong –O–H stretching band, very weak amide I and II band and the shift of –O–H stretch to a lower position from 3304 to 3280 cm^{-1} indicated that the occurrence of cross-linking between hydroxyl groups of PVA with the amide group of collagen might be through a hydrogen bond.^{10,33}

Besides, the IR spectra of PVA/collagen blends doped with different concentrations of B1 showed that the position of amide bands were almost at the same wavenumbers for all the blends, as shown in Figure 4c–g. The different concentrations of the B1-doped PVA/collagen composite film also gave strong –O–H stretching bands with a shift from high frequency to low frequency. This indicated there could be a hydrogen bonding between the dopant and matrix. The bands at 2922 cm^{-1} are related to the stretching of the aliphatic –C–H group. The vibration of the aromatic ring was observed at 1610–1570 cm^{-1} . The band at 1680 cm^{-1} corresponded to carbonyl stretching vibration for the α , β unsaturated keto group. No further variation was observed in PVA/collagen/B1 composite films compared with a pure PVA film.³⁴

3.4. Thermogravimetric Analysis. TGA was used to determine the thermal stability of fabricated films. The analysis was carried out in the range of 25–800 °C in the air at a heating rate of 10 °C/min. The thermogram is represented in Figure 5. The thermogram of developed films revealed weight loss which was observed in three stages. From the graph, it could be inferred that below 100–150 °C, all the samples lost water due to the absorption of moisture by the polymer leading to weight loss. For the PVA film, the weight loss (10%) occurred at 190 °C, weight loss (15%) occurred at 260 °C, weight loss (80%) occurred at 432 °C and complete degradation occurred at 700 °C. The first region 100–200 °C could be attributed to the loss of absorbed water molecules. The second region between 200

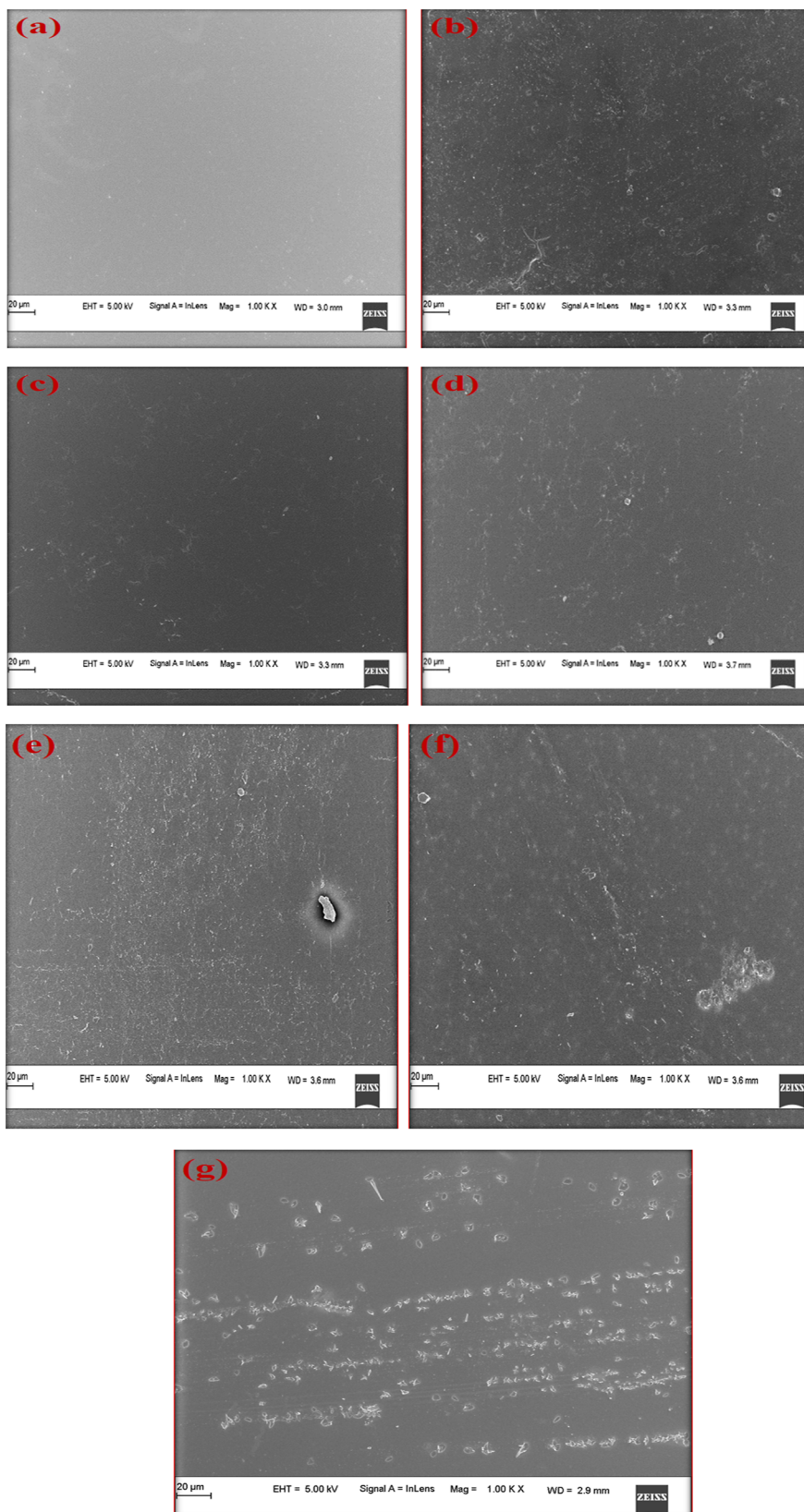


Figure 3. SEM micrographs of PVA/collagen blend films doped with different concentrations of B1: (a) PVA(2%), (b) PVA(2%)/collagen(2%), (c) PVA/collagen/B1(0.25%), (d) PVA/collagen/B1(0.5%), (e) PVA/collagen/B1(1%), (f) PVA/collagen/B1(2%), and (g) PVA/collagen/B1(4%).

and 300 °C related to the loss of water bound to the polymer matrix. The third region between 340 and 400 °C was associated with the decomposition and carbonization of the polymer.

Meanwhile, collagen blended with the PVA film showed weight loss of 15% at 150 °C, weight loss of 20% at 252 °C, weight loss of 90% at 428 °C, and complete degradation was observed at 700

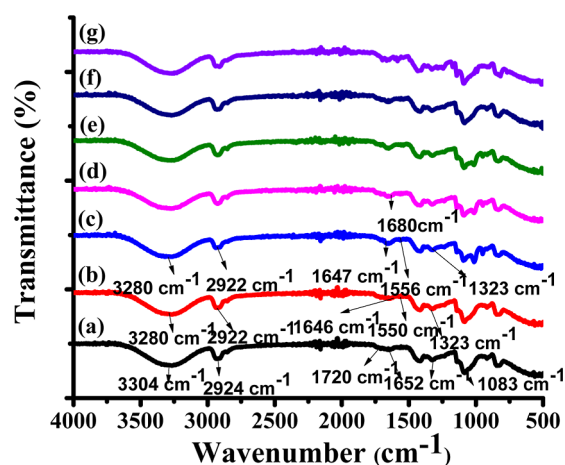


Figure 4. FTIR spectra of PVA/collagen blend films doped with different concentrations of **B1**: (a) PVA(2%), (b) PVA(2%)/collagen(2%), (c) PVA/collagen/B1(0.25%), (d) PVA/collagen/B1(0.5%), (e) PVA/collagen/B1(1%), (f) PVA/collagen/B1(2%), and (g) PVA/collagen/B1(4%).

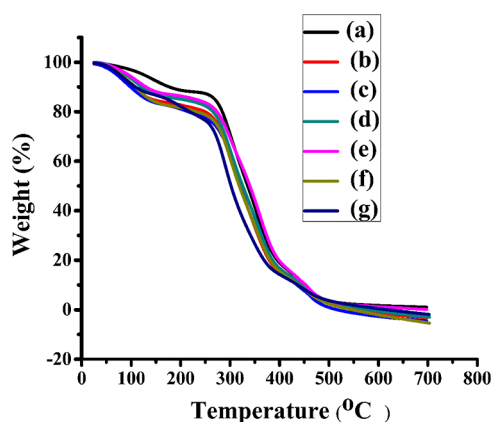


Figure 5. TGA thermograms of PVA/collagen blend films doped with different concentrations of **B1**: (a) PVA(2%), (b) PVA(2%)/collagen(2%), (c) PVA/collagen/B1(0.25%), (d) PVA/collagen/B1(0.5%), (e) PVA/collagen/B1(1%), (f) PVA/collagen/B1(2%), and (g) PVA/collagen/B1(4%).

°C. The films with different concentrations of **B1** doped into the PVA/collagen blend showed weight loss of 15% at 145 °C and weight loss of 20% at 260 °C. The decomposition of weight loss of 15–20% was observed at around 145–260 °C. Upon heating of the PVA/collagen blend, the major changes could be attributed to collagen. The collagen undergoes denaturation leading to conformational changes upon heating. Breaking of various cross-links by nonenzymatic glycosylation of lysine and hydroxylysine at the intermolecular level, where as at intra-

molecular level it caused the breaking of the disulfide bridge. The hydrogen bonded water molecule would be released, causing the collapse of the triple-helical structure. All these phenomena caused by heating would result in a random fragmentation of a larger molecule into smaller ones with the reduction in banding periodicity ($D = 38 \pm 10$ nm) of collagen on heating over 100 °C. This phenomenon occurred due to the breaking of cross-links. The unfolding took place at a thermally less stable domain located in gap regions.³⁵ This caused reduced banding periodicity while maintaining the ultrastructure intact. Major degradation, 91% of weight loss occurred at 444 °C, indicating the production of gaseous elements, and complete degradation at 700 °C.

3.5. Mechanical Properties. The variation in the mechanical properties of the fabricated composite films is shown in Table 2. The addition of different concentrations of **B1** increased Young's modulus (146–317 MPa). Tensile strength decreased initially for PVA/collagen and PVA/collagen/**B1** (0.25%) and then increased from (23.3–39.21 MPa) and decreased its elongation at break (158.8–105.2%). The crystallites could be formed by the interchain H-bonding between PVA and collagen increased the crystallinity of the matrix (Figure 1a,b) which lead to internal friction in the matrix. Many hydroxyl groups present on the surface of the PVA could easily form hydrogen bonds with other polymers.^{36,37} The glycine, proline, and hydroxyproline are the three major amino acids present in collagen responsible for hydrogen bonding.²⁰ The presence of **B1** further enhanced the crystalline nature by network of hydrogen bonds formed between the $-C=O-$ and $-N-H$ of the dopant and amide linkage of collagen as well as $-O-H$ of PVA, respectively,³⁸ witnessing an increase in Young's modulus and a decrease in the elongation at break of composite films. The tensile strength of the composite film (PVA/collagen/**B1**) was much higher than those of the pure PVA film and PVA/collagen films, which indicated that the introduction of **B1** into the matrix; could stack to form crystallite regions played a key role in the enhancement of the toughness of films.^{30,39,40}

3.6. Density of the Cross-Linked Composite Film. As the concentration of **B1** increased, so the density of all cross-linked films were increased, as shown in Figure 6. The addition of collagen as well as **B1** into the PVA matrix increased the density of films due to interchain interactions resulting in rigid regions in the matrix which was also evidenced in SEM images (Figure 3). The analysis further confirmed that a higher crosslinking density lead to a higher Young's modulus.⁴¹

3.7. UV–Vis Spectral Analysis. Basically, the PVA film was transparent to UV radiation. The collagen absorbed at a wavelength of 225 nm. The addition of different concentrations of **B1** to the PVA/collagen matrix as a dopant shifted its λ_{max} 370 to 390 nm in the UV-A (320–400 nm) region, as shown in

Table 2. Mechanical Property of the Fabricated Composite Films

S. no.	Samples	Young's modulus (MPa)	Tensile strength (MPa)	Elongation at break (%)	Stress at break (MPa)	Thickness (mm)
1.	PVA	146	23.3	158.8	14.8	0.071
2.	PVA/collagen	186	18.0	155.3	4.38	0.062
3.	PVA/collagen/B1(0.25%)	199	16.6	145.7	6.45	0.070
4.	PVA/collagen/B1(0.5%)	201	28.7	135.0	4.9	0.080
5.	PVA/collagen/B1(1%)	270	31.0	129.2	5.54	0.097
6.	PVA/collagen/B1(2%)	299	35.2	111.1	5.21	0.062
7.	PVA/collagen/B1(4%)	317	39.21	105.2	5.05	0.046

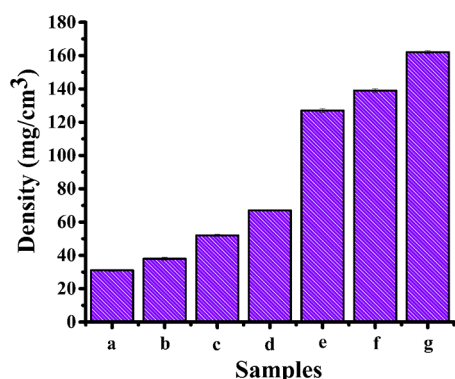


Figure 6. Density of the cross-linked composite film, the columns represent the mean \pm SEM of seven independent experiments: (a) PVA(2%), (b) PVA(2%)/collagen(2%), (c) PVA/collagen/B1(0.25%), (d) PVA/collagen/B1(0.5%), (e) PVA/collagen/B1(1%), (f) PVA/collagen/B1(2%), and (g) PVA/collagen/B1(4%).

Figure 7. The bathochromic shift caused by the intercalation of B1 into the matrix. The absorption maxima were influenced by

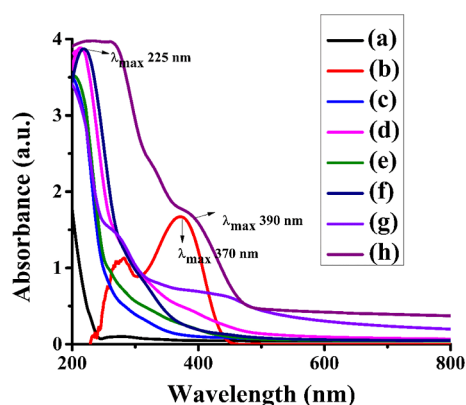


Figure 7. UV spectra analysis of PVA/collagen blend films doped with different concentrations of B1: (a) PVA(2%), (b) B1, (c) PVA(2%)/collagen(2%), (d) PVA/collagen/B1(0.25%), (e) PVA/collagen/B1(0.5%), (f) PVA/collagen/B1(1%), (g) PVA/collagen/B1(2%), and (h) PVA/collagen/B1(4%).

the strong interaction between matrix and dopant by a hydrogen bond resulting in the alteration of molecular packing.⁴² Carbonyl compounds show both π to π^* (intense and shorter wavelength) and n to π^* (less intense and longer wavelength) transitions. The bathochromic shift might be attributed to (i) possible intermolecular hydrogen bonding between $-C=O-$ of the dopant and $-O-H$ of the polymer chain and (ii) the bathochromic shift of about 20 nm was observed upon the

addition of the dopant could be due to the J aggregate formation of dopants in the polymer matrix. The large dipole moment associated with the piperidone ring influenced head-to-tail alignment with +I effect. It was observed that the presence of the electron-donating $-SCH_3$ group enhanced the bathochromic effect due to long-range polarization.^{17,18,43} However, increasing the concentration of B1 in the matrix increased the extent of absorption intensity (hyperchromism) at 390 nm as it was evident with crystals of B1 uniformly embedded in the PVA/collagen matrix as it was reflected in SEM images (Figure 3).

3.7.1. Sun Protection Factor (SPF) and Ultra Protection Factor (UPF). At what percentage a material can protect against UV rays was determined by the *in vitro* calculation of SPF. It provides the capability of the material to protect against only UV-B radiation. The UPF is one of the important parameters used to measure the UV-blocking capability of materials. It provides capacity for both UV-A and UV-B protection. These tests are fast, reliable, and economically feasible methods based on UV spectral transmission measurements and have no UV dosage cumulating response. Higher SPF and UPF values result in effective materials that prevent sunburn.⁴⁴ Values between 15 and 30% have been suggested as good, as it indicates that these agents can block 93–97% UV radiation, whereas values > 50% are capable of blocking about 98% UV radiation.²³

3.7.1.1. In vitro SPF Determination of Fabricated Films. An *in vitro* method of determining SPF of the fabricated films was calculated through the UV absorbance value by using the Mansur equation, as shown in Table 3. The SPF of the pure PVA film was obtained 0.794. When it was blended with collagen, the SPF value was found to be 2.968. The B1 alone exhibited an SPF value of 9.003. When the blend film was fabricated with B1, the implication was an increase in SPF values proportional to dopant concentration. The SPF values were found to be in range of 5.41–27.53. The higher the SPF, the more effective the product is in preventing sunburn. The PVA/collagen/B1 (4%) composite film filters 96.37% of UV-B light. Therefore, PVA/collagen/B1 composite films might protect the skin from the harmful effects of the sun. It is also noteworthy that an additional property of probable tyrosinase activity inhibition by B1 synergistically improved the utility of these combinations in skincare products.

3.7.1.2. In vitro UPF Determination of Fabricated Composite Films. The UPF value calculated for the films according to the formulae described in the previous section is represented in Table 3.

The UPF value of the pure PVA film was obtained as 0.034. When it was blended with collagen, the UPF value enhanced 5.71. However, PVA/collagen/B1 films were prepared there was an increase in UPF values (7.01 to 58.23) with respect to the increase in concentration of the dopant, as indicated in Table 3.

Table 3. The SPF and UPF Values of Developed Composite Films

S.no.	Samples	% blocking		SPF	UVP (%)	UPF	UPF ratings
		UVA	UVB				
1.	PVA	12.63	16.15	0.79	nil	0.03	Nonrateble
2.	PVA/collagen	31.21	71.34	2.96	66.30	5.71	Nonrateble
3.	PVA/collagen/B1 (0.25%)	65.98	92.43	5.41	81.55	7.01	Nonrateble
4.	PVA/collagen/B1 (0.5%)	85.77	96.18	9.33	89.29	18.38	Good protection
5.	PVA/collagen/B1 (1%)	66.09	97.07	9.57	89.56	22.50	Moderate protection
6.	PVA/collagen/B1 (2%)	90.23	99.75	9.75	89.75	48.09	Excellent protection
7.	PVA/collagen/B1 (4%)	98.07	99.97	27.53	96.37	58.23	Excellent protection

The higher the UPF, the more effective the product is in filtering sunrays. Moreover, UPF ratings of the composite film [PVA/collagen/B1 (4%)] reached the highest level (50+) [AS/NZS 4399-1996 standard]. The PVA/collagen/B1 (4%) fabricated film showed a higher UPF value of 58.23, which could protect 98% of UV-A light. Therefore PVA/collagen/B1 (4%) fabricated films might protect the skin from harmful effects of the sun as well as fabrics. These composite films could also be used as a packaging material for cosmetics also.

3.8. In vitro vDNA Degradation Study of the Fabricated Composite Films. Even though chemical filters offer better UV absorption range they often suffer from a toxic effect; hence, their use in cosmetics might be restricted. In the present study, fabricated films rated for excellent protection factors especially with 4% dopant combination. The toxic effect might prove to be a disadvantage for applications. Hence, the assay to test the capacity of these fabricated composite films against DNA degradation was carried out on PBR322 DNA. The DNA degradation studies were usually carried out by agarose gel electrophoresis, as shown in Figure 8. The smearing band

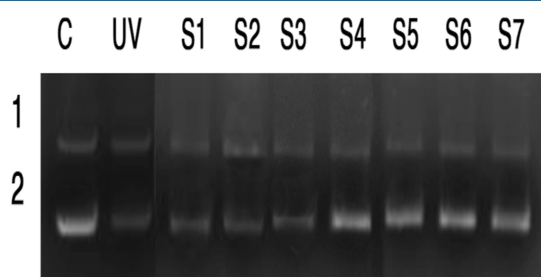


Figure 8. DNA protection study of PVA/collagen blend film doped with different concentrations of B1: Lane 1 (C) shows control PBR322 DNA without photo-irradiation and Lane 2 (UV) shows control PBR322 DNA subjected to photo-irradiation (S1) PVA(2%), (S2) PVA/collagen(2%), (S3) PVA/collagen/B1(0.25%), (S4) PVA/collagen/B1(0.5%), (S5) PVA/collagen/B1(1%), (S6) PVA/collagen/B1(2%), and (S7) PVA/collagen/B1(4%).

produced during electrophoresis indicated the DNA degradation.⁴⁵ Lane 1(C) is the control PBR322 DNA without photo-irradiation showed intact supercoiled form, which confirmed there was no photocleavage occurred. Lane 2 (UV) is the control PBR322 DNA subjected to photo-irradiation showed a diminishing supercoiled band due to photocleavage. Lanes S1 to S3 containing PVA, PVA/collagen blend film, and PVA/collagen blend film with 0.25% B1 showed specific UV-irradiated DNA which also clearly showed the diminished visibility of DNA band (number 2) including loss of DNA integrity. It clearly showed that there is a possibility of DNA photocleavage. In the case of Lanes S4 to Lane S7, containing PVA/collagen blend film with the increase in concentrations of B1 (0.5–4%), showed similar results compared to the control (C), and the resultant DNA showed an intact supercoiled form of DNA as separate clear two bands (Figure 8). The DNA damage could occur when DNA directly absorbs a UV-B photon. The UV-B light causes the formation of thymine dimers which bond together into pyrimidine dimers, leads to the disruption in the strand, the enzymes cannot copy, and the cell cannot carry out its normal functions. It causes sunburn, triggering the production of melanin. This incorrect repair or a missed dimer could lead to cancerous cells formation. The obtained results indicated that the DNA is protected against UV

radiation with the PVA/collagen blend film with the increase in concentrations of B1. The composite films exhibited enhanced UPF values upto 58.23. Among tested films, the composite film with B1 (4%) dopant emerged as the best one to protect against UV rays with effective inhibition of DNA degradation, proving the nontoxic nature of composite films.

4. CONCLUSIONS

The composite films fabricated by PVA/collagen doped with B1 turned out to be excellent UV filtering materials with a dopant-dependent change in SPF (5.41 to 27.53) and UPF (7.01 to 58.23) values. The film with 4% dopant B1 had showed the highest SPF and UPF values. The inhibition of DNA degradation by these films under UV irradiation would make these films as excellent nontoxic UV filtering materials. This study also indicated the cosmeceutical value of fabricated films.

AUTHOR INFORMATION

Corresponding Author

Balladka Kunhanna Sarojini – Department of Industrial Chemistry, Mangalore University, Mangalore 574199 Karnataka, India; orcid.org/0000-0001-8193-1138; Phone: +91 9886273404 (M); Email: bksaroj35@gmail.com

Authors

Niveditha Nagappa Bailore – Department of Biochemistry, Mangalore University, Mangalore 574199 Karnataka, India
Kishori Ramachandra Harshitha – Department of Industrial Chemistry, Mangalore University, Mangalore 574199 Karnataka, India

Complete contact information is available at:

<https://pubs.acs.org/10.1021/acsomega.2c00772>

Notes

The authors declare no competing financial interest.

ACKNOWLEDGMENTS

The authors would like to acknowledge DST-PURSE and University Science Instrumentation Centre (USIC), Mangalore University for providing the SEM, TGA, UV spectral analysis, and FTIR facilities.

REFERENCES

- Soon-Do, Y.; Mi-Hwa, P.; Hun-Soo, B. Mechanical and water barrier properties of starch/PVA composite films by adding nano-sized Poly(Methyl Methacrylate-Co-Acrylamide) particles. *Carbohydr. Polym.* **2012**, *87*, 676–686.
- Bari, E.; Sistani, A.; Morrell, J. J.; Pizzi, A.; Akbari, M. R.; Ribera, J. Current strategies for the production of sustainable biopolymer composites. *Polym* **2021**, *13*, 2878.
- Pereira, V. A.; de Arruda, I. N. Q.; Stefani, R. Active chitosan/PVA films with anthocyanins from Brassica Oleraceae (Red Cabbage) as time-temperature indicators for application in intelligent food packaging. *Food Hydrocolloids* **2015**, *43*, 180–188.
- Tanase, E. E.; Popa, M. E.; Rapa, M.; Popa, O. Preparation and characterization of biopolymer blends based on polyvinyl alcohol and starch. *Rom. Biotechnol. Lett.* **2015**, *20*, 10307–10315.
- <https://www.gminsights.com/industry-analysis/fish-collagen-peptides-market>, accessed 8/4/2022.
- Bailore, N. N.; Sarojini, B. K.; Pushparekha; Kabiru, B. Customized eco-friendly UV-B filtering films from vital collagen isolated from Arabian Sea fish Indian oil sardine (*Sardinella longiceps*). *AIP Conf. Proc.* **2020**, *2244*, 020003.

- (7) Quintana Lazópulos, S. Q.; Svarc, F.; Sagrera, G.; Dixelio, L. Absorption and photo-stability of substituted dibenzoylmethanes and chalcones as UVA filters. *Cosmetics* **2018**, *5*, 33.
- (8) Reddy, M. S. B.; Ponnamma, D.; Choudhary, R.; Sadasivuni, K. K. A comparative review of natural and synthetic biopolymer composite scaffolds. *Polym* **2021**, *13*, 1105.
- (9) Sionkowska, A. Current research on the blends of natural and synthetic polymers as new biomaterials: Review. *Prog. Polym. Sci.* **2011**, *36*, 1254–1276.
- (10) Perkasa, D. P.; Erizal, E.; Abbas, B. Polymeric Biomaterials Film Based on Poly(vinyl Alcohol) and Fish Scale Collagen by Repetitive Freeze-thaw Cycles Followed by Gamma Irradiation. *Indones. J. Chem.* **2013**, *13*, 221–228.
- (11) Bukhari, S. N. A.; Jantan, I.; Unsal Tan, O.; Sher, M.; Naeem-ul-Hassan, M.; Qin, H. L. Q. Biological Activity and Molecular Docking Studies of Curcumin-Related α,β -Unsaturated Carbonyl-Based Synthetic Compounds as Anticancer Agents and Mushroom Tyrosinase Inhibitors. *J. Agric. Food Chem.* **2014**, *62*, 5538–5547.
- (12) Darshan Raj, C. G.; Sarojini, B. K.; Bhanuprakash, V.; Yogisharadhya, R.; Kumara Swamy, B. E. K.; Raghavendra, R. Studies on radioprotective and antiviral activities of some bischalcone Derivatives. *Med. Chem. Res.* **2012**, *21*, 2671–2679.
- (13) Darshan Raj, C. G.; Sarojini, B. K.; Ramakrishna, M. K.; Ramesh, S. R.; Manjunatha, H. In vivo peritoneal antiangiogenesis and *in vitro* antiproliferative properties of some bischalcone derivatives. *Med. Chem. Res.* **2012**, *21*, 453–458.
- (14) Mayekar, A. N.; Li, H.; Yathirajan, H. S.; Narayana, B.; Kumari, N. S. Synthesis, characterization and antimicrobial study of some new cyclohexenone derivatives. *Int. J. Chem.* **2010**, *2*, 114–123.
- (15) Harshitha, K. R.; Sarojini, B. K. Donor-Acceptor-Donor (DAD) type pipyridinonyl bischalcone derivatives as promising UVA Filters. *AIP Conf. Proc.* **2020**, *2244*, 040001.
- (16) Rashmi, M.; Indira, J.; Sarojini, B. K.; Mohan, B. J.; Joe, I. H.; Aswathy, P. Ultrafast nonlinear optical properties of cyclohexenone carboxylate derivatives and their application as organic saturable absorbers. *Opt. Laser Technol.* **2021**, *139*, 106902.
- (17) Pai, A. J.; Sarojini, B. K.; Harshitha, K. R.; Shivarama Holla, B.; Lobo, A. G. Spectral, morphological and optical studies on bischalcone doped polylactic acid (PLA) thin films as luminescent and UV radiation blocking materials. *Opt. Mater.* **2019**, *90*, 145–151.
- (18) Pai, A. J.; Sarojini, B. K.; Harshitha, K. R.; Soldera, A. Environmentally Benign Blue Emissive Films from Host-Dopant Interaction of PLA-Bischalcone Combination with High UV Endurance. *J. Polym. Environ.* **2021**, *30*, 373.
- (19) Harshitha, K. R.; Sarojini, B. K.; Narayana, B.; Maidur, S. R.; Patil, P. S.; Kumara, K. Donor- π -Acceptor- π -Donor class of 2,5-dibenzylidene-cyclopentan-1-one analogues as efficient third order nonlinear optical and photoluminescent materials - An experimental investigation. *Opt. Laser Technol.* **2019**, *117*, 304–315.
- (20) Niveditha, N. B.; Sarojini, B. K.; Doddapaneni, S. J. D. S. Isolation and biochemical characterization of vital protein collagen: fish waste valorization of Arabian Sea fish *Sardinella longiceps* and Its fluorescence quenching property. *Biomedicine* **2020**, *40*, 36–44.
- (21) Grabska-Zielińska, S.; Sionkowska, A.; Reczyńska, K.; Pamuła, E. Physico-chemical characterization and biological tests of collagen/silk fibroin/chitosan scaffolds cross-linked by dialdehyde starch. *Polym* **2020**, *12*, 372.
- (22) Sionkowska, A.; Michalska, M.; Walczak, M.; Śmiechowski, K.; Grabska, S. Preparation and characterization of silk fibroin/collagen sponge modified by chemical cross-linking. *Mol. Cryst. Liq. Cryst.* **2016**, *640*, 180–190.
- (23) Olayemi, O.; Isimi, C.; Ekere, K.; Gbate, M. A.; Emeje, M. Determination of Sun Protection Factor Number: An emerging *in vitro* tool for predicting UV protection capabilities. *Int. J. Herb. Med.* **2017**, *5*, 6–9.
- (24) Donglikar, M. M.; Deore, S. L. Development and evaluation of herbal sunscreen. *Pharmacogn. J.* **2016**, *9*, 83–97.
- (25) Mali, S. S.; Killedar, S. G. Formulation and *in vitro* evaluation of gel for SPF determination and free radical scavenging activity of Turpentine and Lavender oil. *Pharma Innov. J.* **2018**, *7*, 85–90.
- (26) Khan, M. A. Sun Protection Factor determination studies of some sunscreen formulations used in cosmetics for their selection. *J. Drug Delivery Ther.* **2018**, *8*, 149–151.
- (27) Sadeghifar, H.; Venditti, R.; Jur, J.; Gorga, R. E.; Pawlak, J. J. Cellulose-Lignin biodegradable and flexible UV protection film. *ACS Sustainable Chem. Eng.* **2017**, *5*, 625–631.
- (28) Cunha, C. S.; Castro, P. J.; Sousa, S. C.; Pullar, R. C.; Tobaldi, D. M.; Piccirillo, C.; Pintado, M. M. Films of chitosan and natural modified hydroxyapatite as effective UV-protecting, biocompatible and antibacterial wound dressings. *Int. J. Biol. Macromol.* **2020**, *159*, 1177–1185.
- (29) Wang, Y.; Su, J.; Li, T.; Ma, P.; Bai, H.; Xie, Y.; Chen, M.; Dong, W. A Novel UV-shielding and transparent polymer film: When bioinspired dopamine-melanin hollow nanoparticles join polymers. *ACS Appl. Mater. Interfaces* **2017**, *9*, 36281–36289.
- (30) Wang, Y.; Guo, Z.; Qian, Y.; Zhang, Z.; Lyu, L.; Wang, Y.; Ye, F. Study on the electrospinning of gelatin/pullulan composite nanofibers. *Polymers* **2019**, *11*, 1424.
- (31) Al-Emam, E.; Soenen, H.; Caen, J.; Janssens, K. Characterization of polyvinyl alcohol-borax/agarose (PVA-B/AG) double network hydrogel utilized for the cleaning of works of art. *Herit Sc* **2020**, *8*, 1–14.
- (32) Zhang, X.; Tang, K.; Zheng, X. Electrospinning and rheological behavior of Poly (Vinyl Alcohol)/collagen blended solutions. *J. Wuhan Univ. Technol., Mater. Sci. Ed.* **2015**, *30*, 840–846.
- (33) Huang, C. C. Design and characterization of a bioinspired polyvinyl alcohol matrix with structural foam-wall microarchitectures for potential tissue engineering applications. *Polym* **2022**, *14*, 1585.
- (34) Tay, M. G.; Tiong, M. H.; Chia, Y. Y.; Kuan, S. H. C.; Liu, Z. Q. A way to improve luminescent efficiency of bis-chalcone derivatives. *J. Chem.* **2016**, *2016*, 1–8.
- (35) Bozec, L.; Odlyha, M. Thermal denaturation studies of collagen by microthermal analysis and atomic force microscopy. *Biophys. J.* **2011**, *101*, 228–236.
- (36) Abdullah, Z. W.; Dong, Y.; Davies, I. J.; Barbhuiya, S. PVA, PVA Blends, and Their Nanocomposites for Biodegradable Packaging Application. *Polym.-Plast. Technol. Eng.* **2017**, *56*, 1307–1344.
- (37) Shi, X.; Bao, W. Hydrogen-bonded conjugated materials and their application in organic field-effect transistors. *Front. Chem.* **2021**, *9*, 1–6.
- (38) Yao, B.; Li, N.; Wang, C.; Hou, G.; Meng, Q.; Yan, K. Novel asymmetric 3,5-bis(arylidene)piperidin-4-one derivatives: synthesis, crystal structures and cytotoxicity. *Acta Crystallogr.* **2018**, *74*, 659–665.
- (39) Mirjalili, F.; Yassini Ardekani, A. Preparation and characterization of starch film accompanied with ZnO nanoparticles. *J. Food Process Eng.* **2017**, *40*(). DOI: 10.1111/jfpe.12561.
- (40) Masuelli, M. A. Introduction of fibre-reinforced polymers polymers and composites: concepts, properties and processes. *Fiber reinforced polymers-the technology applied for concrete repair*; IntechOpen, 2013.
- (41) Zhao, J.; Yu, P.; Dong, S. The Influence of Crosslink density on the failure behavior in amorphous polymers by molecular dynamics simulations. *Materials* **2016**, *9*(). DOI: 10.3390/ma9040234.
- (42) Chen, H.; Noirbent, G.; Liu, S.; Brunel, D.; Graff, B.; Gigmes, D.; Zhang, Y.; Sun, K.; Morlet-Savary, F.; Xiao, P.; Dumur, F.; Lalevée, J. Bis-chalcone derivatives derived from natural products as near-UV/Visible light sensitive photoinitiators for 3D/4D printing. *Mater. Chem. Front.* **2021**, *5*, 901–916.
- (43) Zakharova, G. V.; Gutrov, V. N.; Nuriev, V. N.; Zyuz'kevich, F. S.; Vatsadze, S. Z.; Gromov, S. P.; Chibisov, A. K. Effect of substituents on spectral, luminescent, and time-resolved spectral properties of 2,6-Diarylidene derivatives of cyclohexanone. *High Energy Chem.* **2017**, *51*, 424–426.
- (44) Golmohammadzadeh, S.; Imani, F.; Hosseinzadeh, H.; Jaafari, M. R. Preparation, characterization and evaluation of Sun Protective and

moisturizing effects of nanoliposomes containing safranal. *Iran. J. Basic Med. Sci.* **2011**, *14*, 521–533.

(45) Kumsiri, R.; Kanchanaphum, P. Comparison of time course detection of human male DNA from blood stains on various objects on surface in a natural environment and in a laboratory using loop-mediated isothermal amplification (LAMP). *Scientifica* **2021**, *2021*, 1.